JEE Journal of Ecological Engineering

Journal of Ecological Engineering 2022, 23(9), 88–99
https://doi.org/10.12911/22998993/151745
ISSN 2299–8993, License CC-BY 4.0

Received: 2022.06.07
Accepted: 2022.07.08
Published: 2022.08.01

Functionalization of Gold Nanoparticles for the Detection of Heavy Metals in Contaminated Water Samples in the Province of Tayacaja

Hipólito Carbajal-Morán[1*], Jesús M. Rivera-Esteban[2], Claver W. Aldama-Reyna[3], Elsi V. Mejía-Uriarte[4]

[1] Facultad de Ingeniería Electrónica-Sistemas, Instituto de Investigación de Ciencias de Ingeniería, Universidad Nacional de Huancavelica, Jr. La Mar 755, Pampas 09156, Huancavelica, Perú

[2] Instituto de Investigación, Universidad Nacional Autónoma de Tayacaja Daniel Hernández Morillo, Jr. Bolognesi 416-418, Pampas 09156, Huancavelica, Perú

[3] Departamento Académico de Física, Universidad Nacional de Trujillo, Av. Juan Pablo II, Trujillo 13011, La Libertad, Perú

[4] Instituto de Ciencias Aplicadas y Tecnología, Universidad Nacional Autónoma de México, Coyoacán 04510, CDMX, México

* Corresponding author's e-mail: hipolito.carbajal@unh.edu.pe

ABSTRACT

The work consisted in functionalizing gold nanoparticles to analytically detect heavy metals in contaminated water; in Tayacaja-Huancavelica-Peru, using physical method of laser ablation. The 450 mJ/p Nd:YAG was used as a pulsed laser generator for the production of colloids from AuNPs by the top-down approach; the target was a 1 cm x 1.5 cm high purity gold metallic plate with a thickness of 1 mm, inside a 20 ml cuvette of deionized water, containing 5 ml of L-Cysteine ≥ 75% purity. Nanoparticle colloids were characterized by UV-Vis spectroscopy from 200 to 1160 nm range. Using a convex lens, the gold metal plate was ablated by the laser equipment, located 10 cm from the focus; with λ = 1064 nm and λ = 532 nm with energy equivalent to 60.28 mJ/p and 32.99 mJ/p respectively, with a ratio of 2 Hz, for 30 and 60 min. All the samples produced were subjected to the dispersion process by sonication at 40 KHz for one hour. The functionalized nanoparticles presented a resonance displacement of the maximum wavelength peak with respect to the reference at approximately 22.51 nm; consequently, the increase in diameter occurred at 52.10 nm. The sensitive capacity of the functionalized nanoparticles was verified for different concentrations of analytes in water, made up of divalent heavy metal ions Cd^{2+}, Pb^{2+}, and trivalent nonmetal As^{3+}. At a concentration greater than 500 uM, the color of the functionalized nanoparticles turned bluish, due to the presence of positive ions. Therefore, it was stated that the functionalized nanoparticles enable the detection of heavy metals in water by color variation.

Keywords: functionalize, metallic colloids, AuNps-Cys, pulsed laser, water with heavy metals, sonication dispersion.

INTRODUCTION

Heavy metals are naturally found as contaminants in water and are often introduced by anthropogenic activities, becoming a global problem [Briffa et al., 2020]. The main polluting sources are: mining, industrial activity, wastewater, hospital and domestic effluents. Likewise, rainwater that erodes soil and rocks is also a source of heavy metal contamination [Rahman & Singh, 2019]. Cadmium (Cd^{2+}), lead (Pb^{2+}), mercury (Hg^{2+}), copper (Cu^{2+}), nickel (Ni^{2+}) and chromium (Cr^{2+}) are considered the most toxic heavy metals which are dissolved in water, in addition to the non-metallic arsenic (As^{3+}). The ingestion of heavy metals, even in low quantity, causes health problems in humans [Rahman & Singh, 2019].

Heavy metals have a long half-life, do not biodegrade and accumulate in different parts of the body. Therefore, early detection of the trace of

these metals contained in water samples and the environment is necessary [Demirak et al., 2006; Waheed et al., 2018]. There are traditional methods for metal detection such as: atomic absorption spectroscopy, ion chromatography, UV-vis spectroscopy, X-ray fluorescence spectroscopy, among others [Titus et al., 2019]. Apart from the high costs, the limitation of these techniques includes the complicated preparation of samples and with specialized personnel, with periods of concentration, which makes it not applicable to the real-time detection of traces of heavy metals [Ullah et al., 2018].

Nanoparticles of different metals can be obtained by two methods, the first being physical and the second chemical. The first requires special devices, such as laser radiation with controlled frequency and power on a solvent, obtaining plasmons and when the solvent evaporates, solid metallic nanoparticles are obtained [Salam et al., 2022]; the second method are the ones that are frequently used due to the ease of controlling the size, shape, location and distribution of nanomaterials [Shin et al., 2022].

In particular, gold nanoparticles (AuNPs) are of interest due to their applicability in various areas due to their biocompatibility and functionalization with various ligands; they present low toxicity with characteristic optical properties only at the nanoscale [Carbajal-Morán et al., 2022; Naharuddin et al., 2022]. The functionalization of AuNPs consists of the incorporation of biomolecules, such as: amino acids, proteins, antibodies, among others; by chemical and/or physical processes on the surface of metallic nanoparticles [Seth, 2020; Zhang et al., 2021].

L-Cysteine, known as mercaptopropionic amino acid, is found in biofluids; as in plants and human plasma, it is a key molecule for protein synthesis [Arathi et al., 2022]. Especially, functionalizing nanoparticles with L-Cysteine is used in sensors, for the optical detection of heavy metals and specific substances in water [Halkare et al., 2019; Kateshiya et al., 2020]. In the work, L-Cysteine ≥ 97%, manufactured by Sigma Aldrich, was used.

On the basis of what was described above, the purpose of the work was to generate AuNPs by using the physical method based on laser ablation and to develop a functionalization procedure for AuNPs with the amino acid L-Cysteine, for use as a sensor to detect analysis of heavy metals in the samples of contaminated water, at more than 3600 meters above sea level, in the province of Tayacaja.

MATERIALS AND METHODS

The AuNPs were obtained by laser ablation with the high-power Nd: YAG equipment, with a ratio of 2 Hz. For a wavelength of 1064 nm, which corresponds to an irradiance of 450 mJ, for periods of 30 and 60 min the AuNPs were produced;

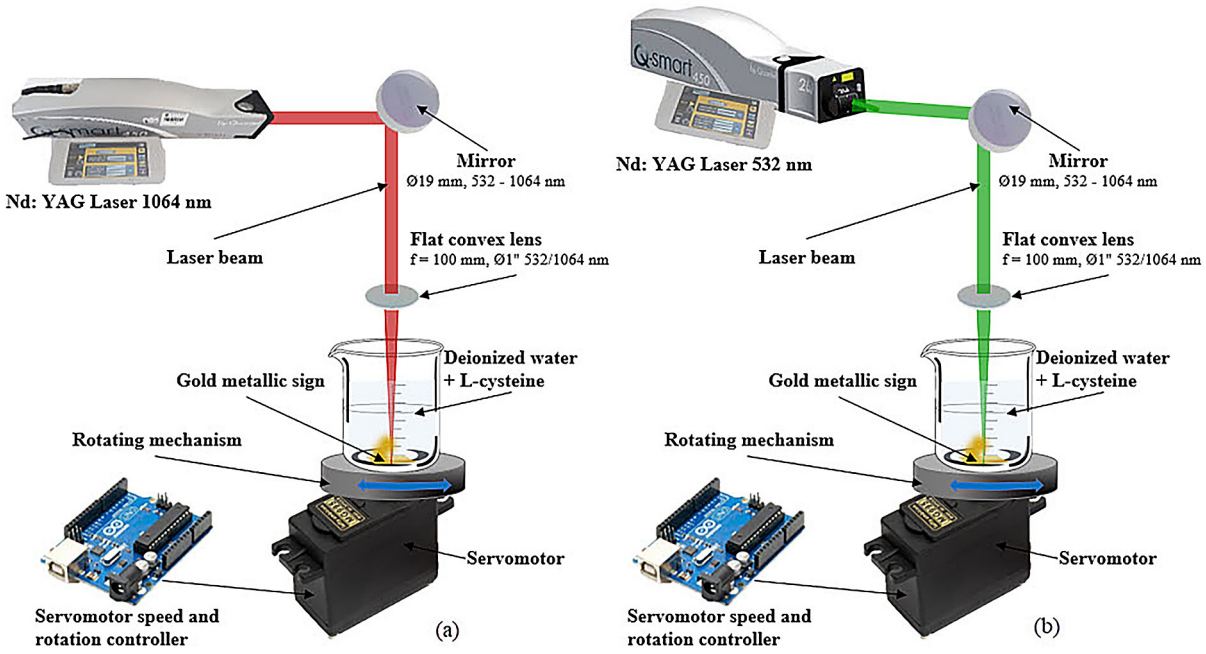

Figure 1. Functionalization diagram of AuNPs with L-Cysteine (a) with 1064 nm laser and (b) with 532 nm laser

likewise, with a wavelength of 532 nm, which corresponds to an irradiance of 220 mJ, the AuNPs were produced for periods of 30 and 60 minutes, using for this, the frequency doubler module for this purpose (2ω) [Quantel, 2019]. The duration of the pulsed laser for all cases was 116 µs.

To functionalize the colloids of AuNPs with the binding L-Cysteine ≥ 97%, the protocol was defined so that functionalization occurs at the time of laser ablation on the 24-carat Au metal plate submerged in 20 ml of deionized water, including 5 ml of L-Cysteine. The ablation was performed with a laser of wavelength λ = 1064 nm and λ = 532 nm for 30 and 60 minutes each. Figure 1 shows the diagram of functionalization processes with lasers of different wavelengths.

During functionalization, the negatively charged amino acid L-Cysteine is attracted to the positively charged gold nanoparticles. To optimize the dispersion in this process, the previously generated colloid was subjected to sonication for one hour, by means of a 40 KHz ultrasound source (see Figure 2).

The functionalized AuNPs were characterized with the UV-Visible-IR spectroscope manufactured by Avantes with λ ranging from 200 nm to 1160 nm; the light source for the detector is deuterium and halogen, with a λ range of 200–1700 nm. The detector reaches up to the value 2048 occupying 64 bits; which allows detecting signals from spectra in the UV and IR range, including filters for deep UV signal measurements. The input connectors are fiber optic FC/PC, the connection to a personal computer (PC) is via USB2, allowing scanning every two milliseconds from the AvaSoft software [Avantes, 2018]. Figure 3 shows the sequence followed for the characterization of the nanoparticles.

The diameter of the non-functionalized (reference) and functionalized nanoparticles was calculated with the mathematical expression of equation 1, based on the λ_{spr} and absorbance of the nanoparticles [Haiss et al., 2007]:

$$d = \frac{\ln\left(\frac{\lambda_{spr} - \lambda_0}{L_1}\right)}{L_2} \quad (1)$$

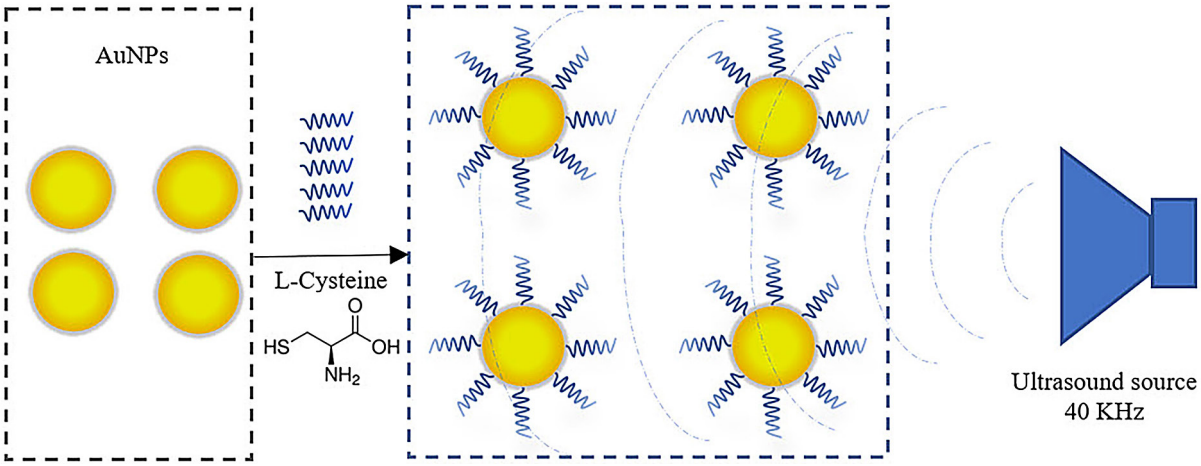

Figure 2. Diagram of the functionalization process of AuNPs with L-Cysteine with sonic dispersion at 40 KHz

Figure 3. Sequence diagram for colloid characterization of functionalized AuNPs

where: $\lambda_0 = 512$ nm, $L_1 = 6.530$ and $L_2 = 0.0216$, with the diameter obtained in equation 1 and the absorbance, the concentration of the nanoparticles is calculated using equation 2. A_{spr} represents the plasmonic resonance peak absorbance, "d" is the diameter of the nanoparticles and c_{Au} concentration of nanoparticles mg/l, considering as experimental values $C_1 = -4.750$ and $C_2 = 0.314$ [Haiss et al., 2007];

$$d = \left(\frac{A_{spr}(5.89 * 10^{-6})}{c_{Au}\exp(C_1)}\right)^{1/C_2} \quad (2)$$

To detect heavy metals in polluted water, the following chemical compounds were used as analyte: 98% cadmium nitrate ($Cd(NO_3)_2$*$4H_2O$), 99.999% lead nitrate for trace metal analysis ($Pb(NO_3)_2$) and formula arsenic oxide of 99.995% for trace analysis (As_2O_3) [Sigma-Aldrich, 2019].

RESULTS AND DISCUSSION

AuNPs colloids were produced by pulsed laser ablation with the Q-Smart 450 equipment, configured for different irradiance powers and ablation periods. With a delay of 116 µs, which is equivalent to 64.04 mJ/p of power, λ = 1064 nm, ratio: 2 Hz, ablation period of 30 min (3600 pulses) and 60 min (7200 pulses), the gold metal plate was irradiated with a rotation by means of a servomotor at 6 rev/min in 20 ml of deionized water, controlled by an Arduino module; reference AuNPs colloids were obtained. When analyzed with a spectrometer, for λ = 532 nm it presented the spectrum of Figure 3, and for λ = 1064 nm it presented the spectrum of Figure 4.

The peak absorbances for the AuNPs in Figure 4 are 523.13 nm and 523.72 nm; from Figure 5 the peak absorbances are 521.95 nm and 522.54 nm. These wavelengths, for different absorbance levels, vary by 1.77 nm, which is not significant; this indicates that the AuNPs obtained have a spherical shape, on average, 23 nm in diameter, which is consistent with that obtained by Kumari and Meena [2020].

Likewise, the nanoparticles are measured by Transmission Electron Microscopy (TEM) at different scales: 2 µm and 50 nm (Figure 6); 100 nm and 200 nm (Figure 7).

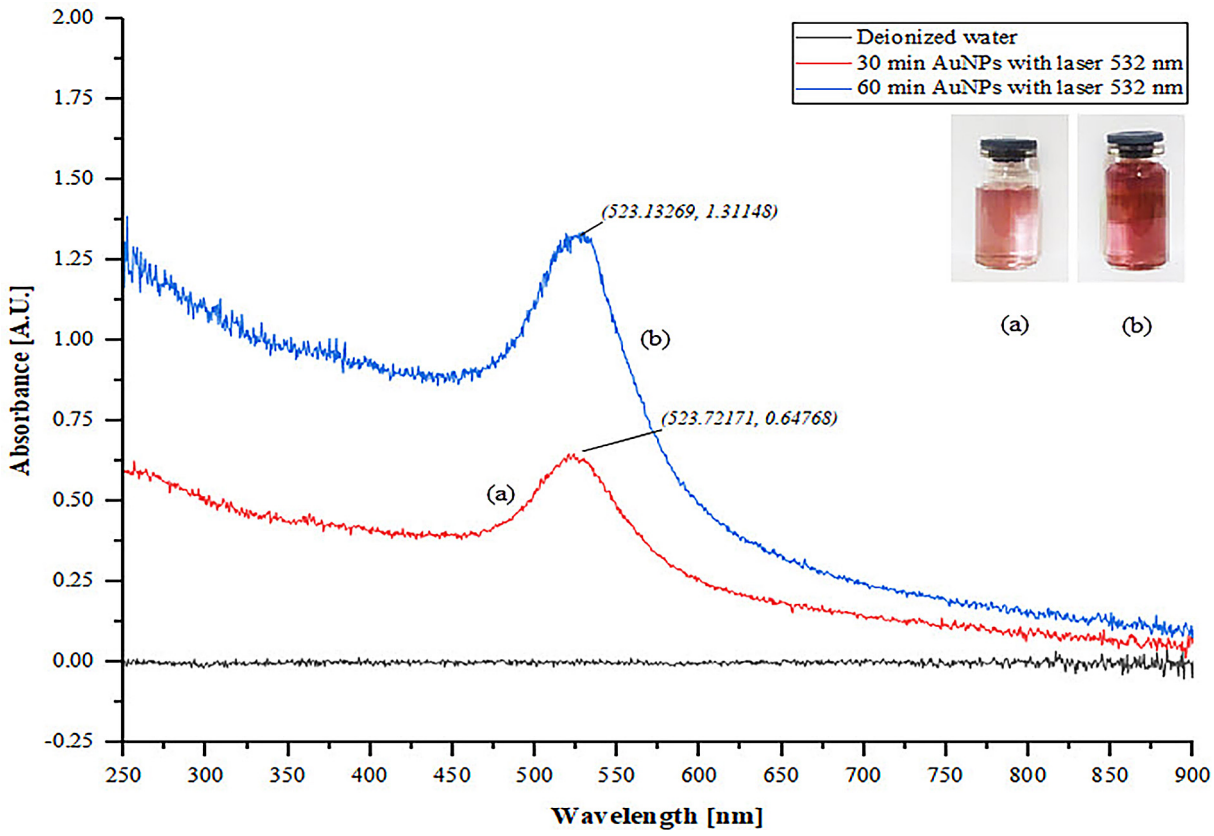

Figure 4. Absorbance spectrum of reference AuNPs produced by wavelength laser ablation wave 532 nm in deionized water (a) for 30 min and (b) for 60 min

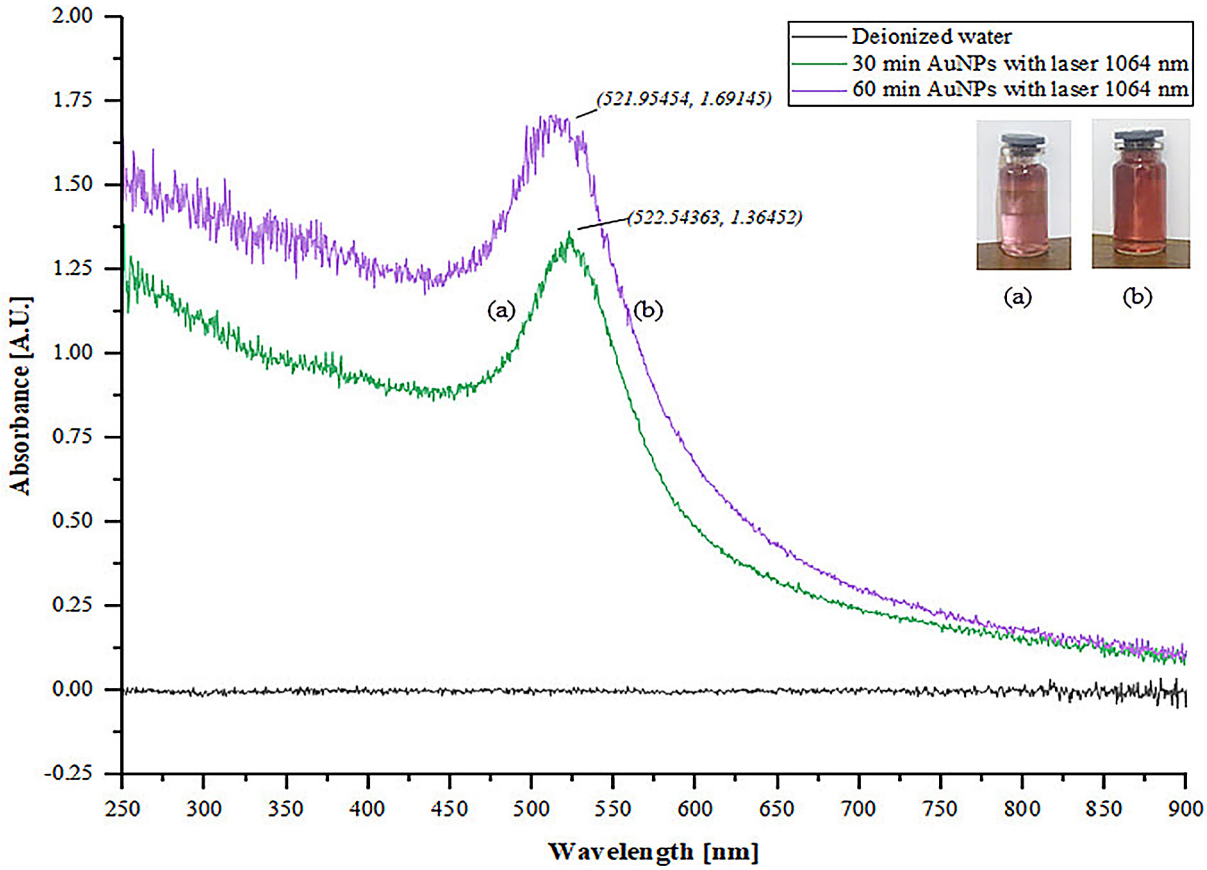

Figure 5. Absorbance spectrum of reference AuNPs, produced by ablation, with wavelength laser 1064 nm in deionized water (a) for 30 min and (b) for 60 min

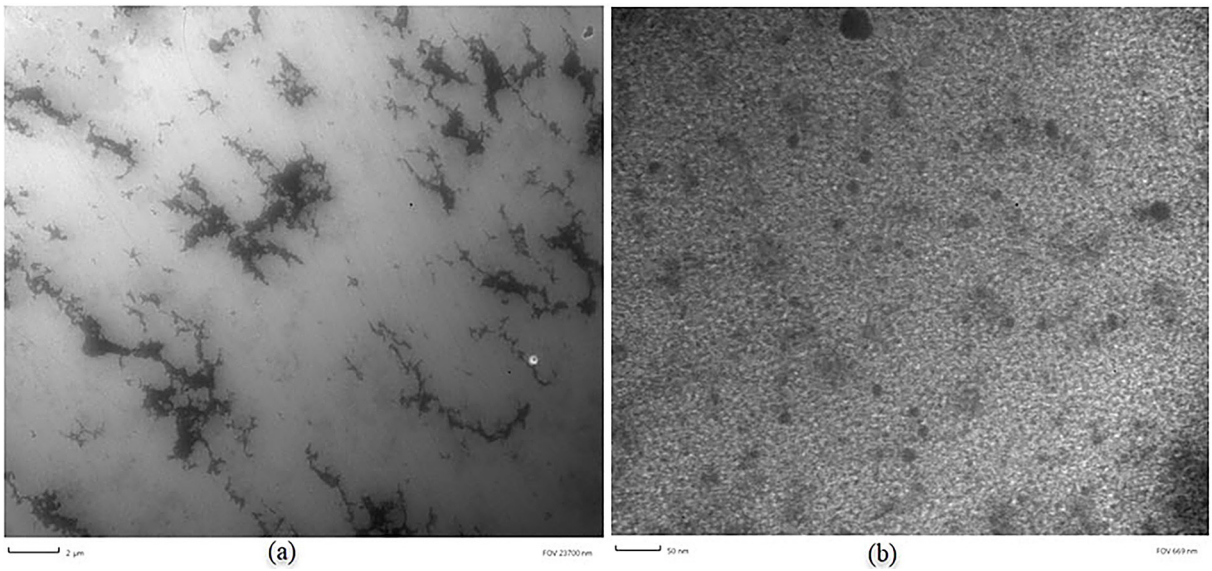

Figure 6. TEM measurement of the reference AuNPs: (a) 2 µm and (b) 50 nm

In figures 6 and 7, the reference nanoparticles present rough surfaces with diameters close to 23 nm, which allows them to be functionalized with L-Cysteine.

With the absorbance and wavelength values obtained from the experiments, the average diameter and concentration of the nanoparticles were determined using equation 3:

$$d = \frac{\ln\left(\frac{\lambda_{spr} - 512}{6.53}\right)}{0.0216} \quad (3)$$

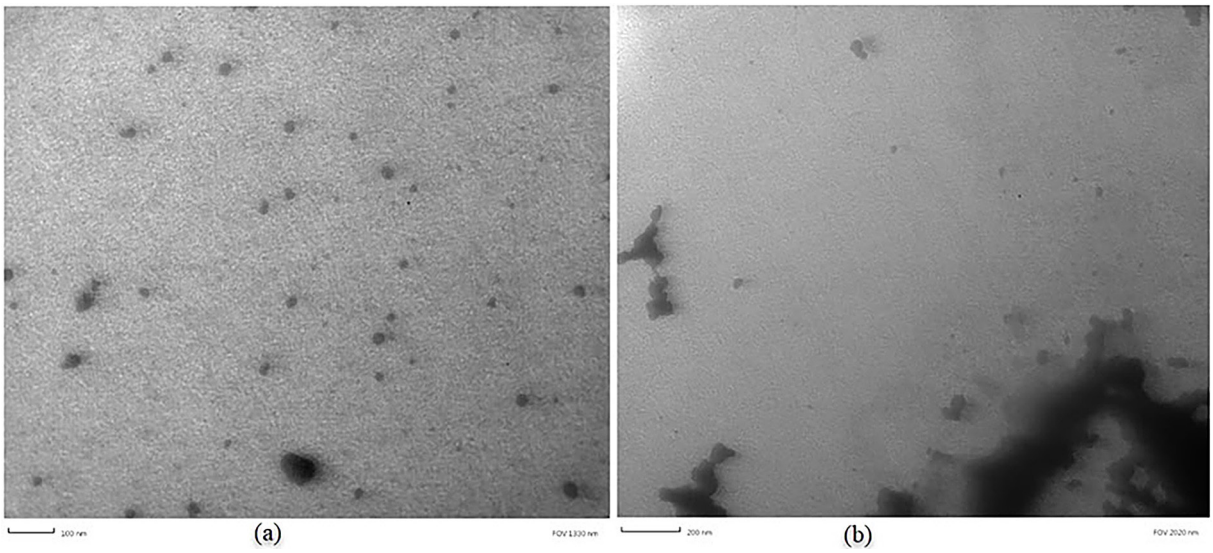

Figure 7. TEM measurement of the reference AuNPs: (a) 100 nm and (b) 200 nm

The concentration of the AuNPs (c_{Au}) dependent on the diameter was calculated with equation 4:

$$c_{Au} = \left(\frac{A_{spr}(5.89 * 10^{-6})}{d * exp(-4.75)}\right)^{1/0.314} \quad (4)$$

Table 1 shows, based on the data found in Figures 4 and 5, the wavelengths of the laser, generation time of nanoparticles, absorbance and wavelengths of the nanoparticles in maximum peaks. Replacing these data in equations "3" and "4", the values corresponding to the diameter and concentration of the reference AuNPs are obtained. It is noted that the average maximum peak wavelength is 522.84 nm; which indicates that they are spherical AuNPs with an average diameter of 23.37 nm.

The gold nanoparticles were functionalized with the amino acid L-Cysteine in the same process of generating the nanoparticles. For this process, for each experiment, 5 ml of previously diluted L-Cysteine was added to 15 ml of pure deionized water obtaining a total of 20 ml of liquid, on which the high purity gold metal plate was placed for its irradiation with a laser of wavelengths of 532 nm and 1064 nm for 30 min and 60 min. As a result, the spectra that are presented in Figures 8, 9, 10 and 11 where obtained. These Figures graphically compare the absorbance and wavelength of the spectrum generated by the reference gold nanoparticles and the gold nanoparticles functionalized with L-Cysteine.

All functionalization processes were carried out at a temperature of 13 °C; which is characteristic in the optics and lasers laboratory of the Faculty of Electronic Engineering and Systems of the UNH, located more than 3600 meters above sea level in the province of Tayacaja-Huancavelica-Peru.

On the basis of the experimental data obtained in Figures 8, 9, 10 and 11, Table 2 presents the wavelengths of the laser, generation time of functionalized and non-functionalized nanoparticles, the wavelengths of the nanoparticles in maximum peaks, the values of the diameters and the differences between them. The diameter of the functionalized AuNPs increased by approximately 52.10 nm, due to the adhesion of the ligand (L-Cysteine) to the surface of the AuNPs.

Table 1. Diameter and colloid concentration of non-functionalized AuNPs

Laser wavelength (nm)	Time (min)	Absorbance in maximum peak (A.U.)	Wavelength at maximum peak (nm)	Diameter (nm)	Concentration (mg/l)
532	30	0.65	523.72	27.08	1.03
	60	1.31	523.13	24.70	1.37
1064	30	1.36	522.54	22.18	1.92
	60	1.69	521.95	19.52	2.88
Average			522.84	23.37	

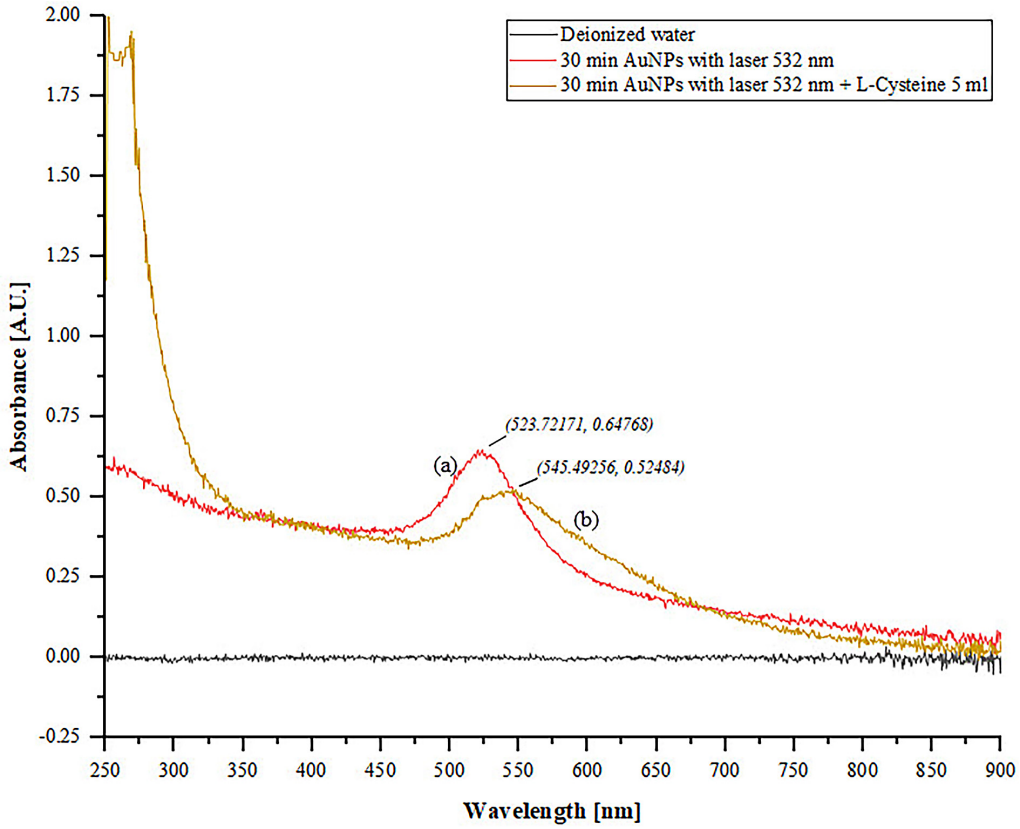

Figure 8. Absorbance spectra of AuNPs, produced by 532-nm laser ablation: (a) non-functionalized and (b) functionalized with 5 ml of L-Cysteine in deionized water in 30 min

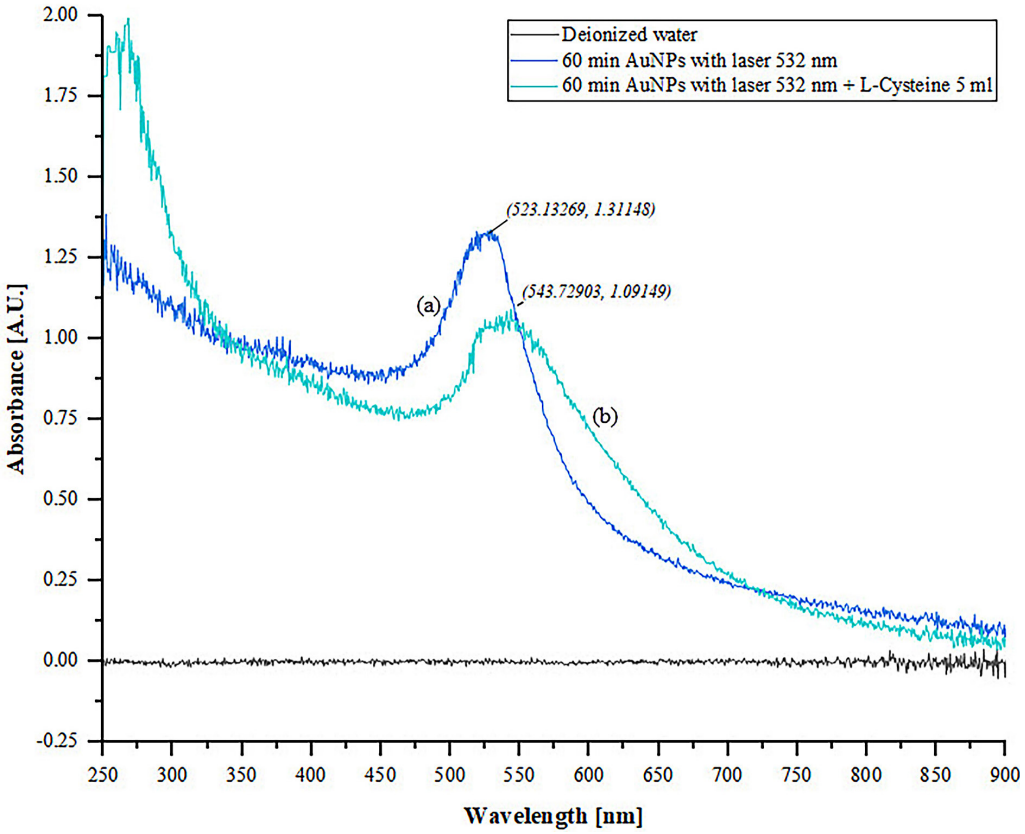

Figure 9. Absorbance spectra of AuNPs, produced by 532 nm laser ablation: (a) non-functionalized and (b) functionalized with 5 ml of L-Cysteine in deionized water in 60 min

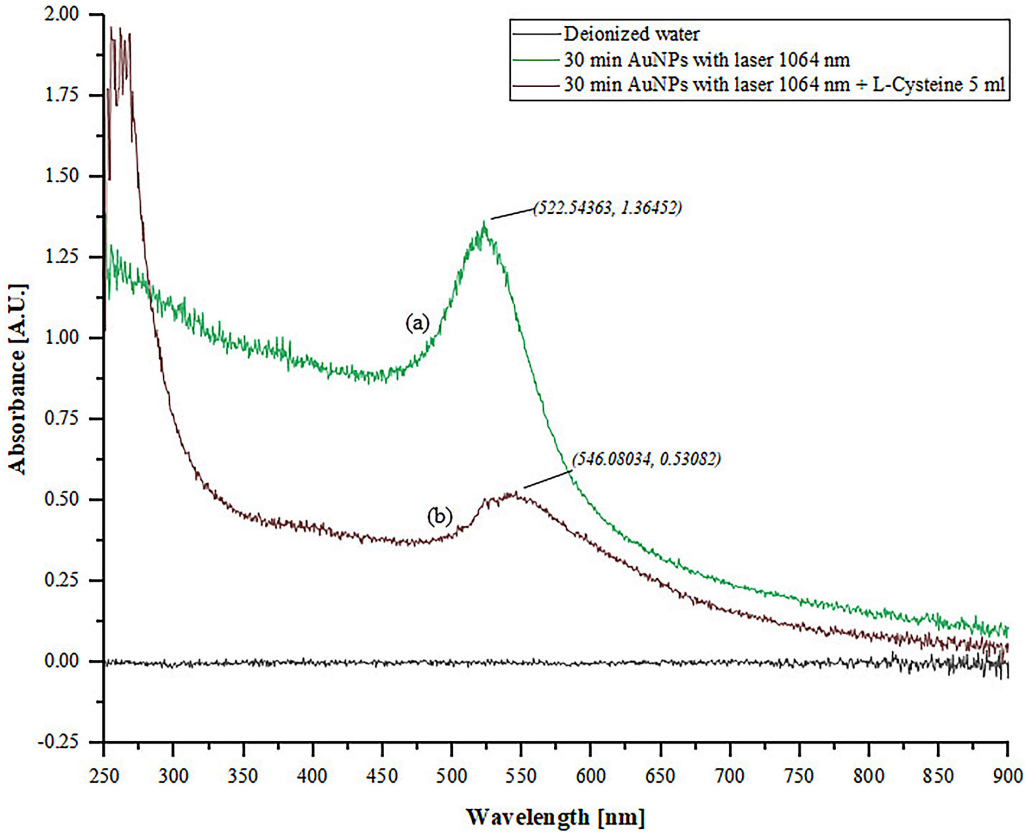

Figure 10. Absorbance spectra of AuNPs, produced by 1064 nm laser ablation: (a) non-functionalized and (b) functionalized with 5 ml of L-Cysteine in deionized water in 30 min

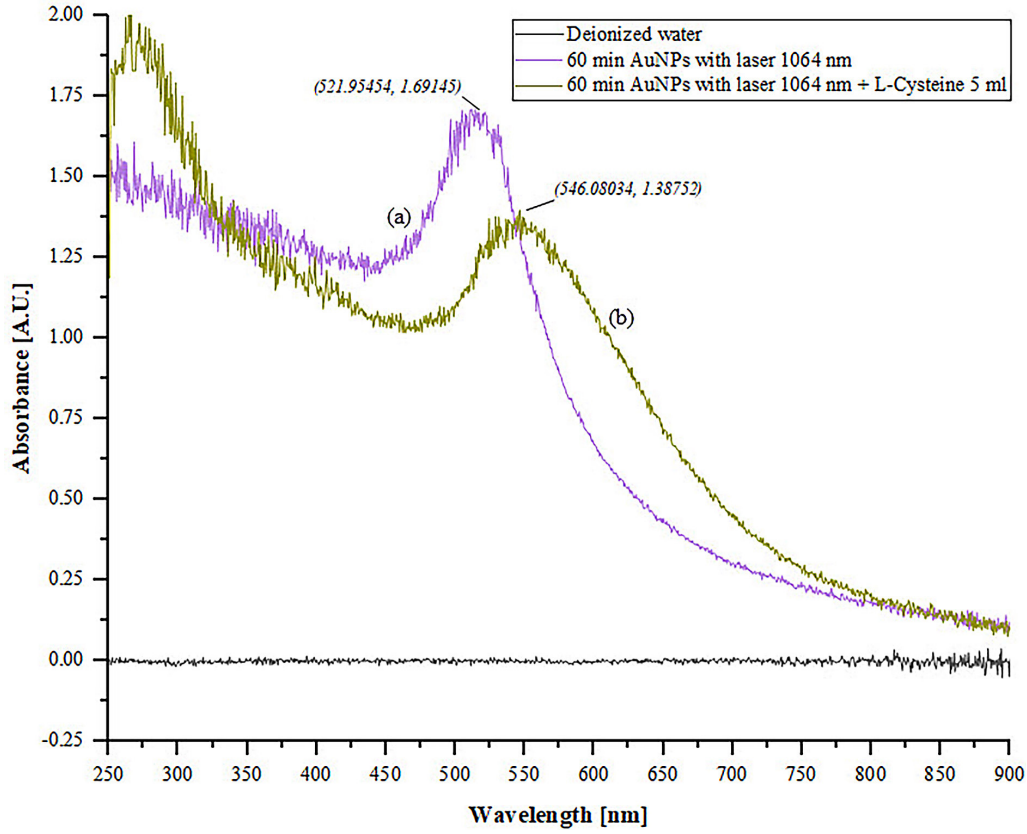

Figure 11. Absorbance spectra of AuNPs, produced by 1064 nm laser ablation: (a) non-functionalized and (b) functionalized with 5 ml of L-Cysteine in deionized water in 60 min

Table 2. Wavelengths at maximum peaks and average diameters calculated for AuNPs in colloidal state non-functionalized and functionalized with L-Cysteine

Laser wavelength (nm)	Time (min)	Maximum peak wavelength of the spectrum of non-functionalized AuNPs (nm)	Maximum peak wavelength of the spectrum of non-functionalized AuNPs (nm)	Diameter of non-functionalized AuNPs (nm)	Diameter of functionalized AuNPs (nm)	Diameter increase (nm)
532	30	523.72	545.49	27.08	75.69	48.61
	60	523.13	543.73	24.70	73.19	48.49
1064	30	522.54	546.08	22.18	76.50	54.31
	60	521.95	546.08	19.52	76.50	56.98
Average		522.84	545.35	23.37	75.47	52.10

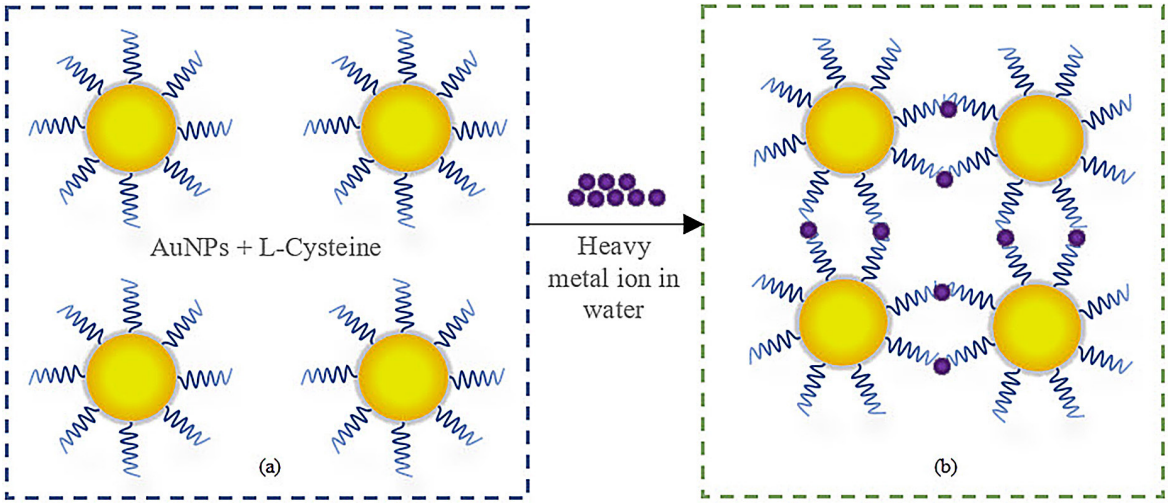

Figure 12. (a) AuNPs functionalized with L-Cysteine, (b) interaction of the functionalized nanoparticles with heavy metal ions in water

Once the functionalized nanoparticles have been obtained, the autors proceeded with the study of the sensitivity in the presence of divalent and trivalent ions in water, analytically. From Figure 12, the binding element that is L-Cysteine encapsulated the nanoparticles (Figure 12a); and in the presence of metal ions in water, the interaction is generated (Figure 12b) [Awual et al., 2015].

The electrons of the functionalized AuNPs are relieved by the presence of analyte ions, altering their optical properties of plasmon resonance, due to the aggregation of elements in the nanoparticle, for which it undergoes color changes (see Figure 13). In addition, the surface potential of the plasmon undergoes changes generating negative potentials of up to -41.2 mV, which was determined by Tripathi et al. [2019].

Amino acids, such as L-Cysteine, are not selective for a particular metal ion [Darbha et al., 2008; Slocik et al., 2008]. To determine the sensitivity of functionalized AuNPs colloids, they were tested with various metal ions, initially with concentrations of 50 µM and 100 µM divalent metal ions Cd^{2+}, Pb^{2+} and the trivalent nonmetal ion As^{3+}; the color of the 10 ml functionalized nanoparticles remained at the initial color without significant changes. With 250 µM Cd^{2+}, Pb^{2+} and As^{3+}; the color of functionalized nanoparticles for

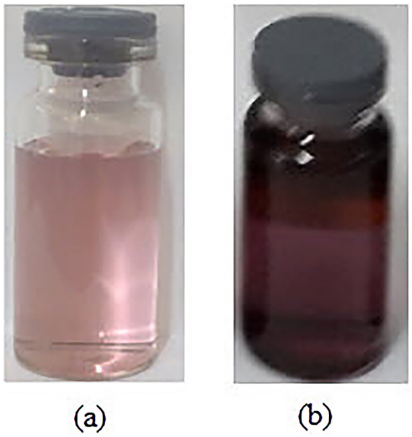

Figure 13. (a) AuNPs + L-Cysteine and (b) AuNPs + L-Cysteine with analyte ion interactions

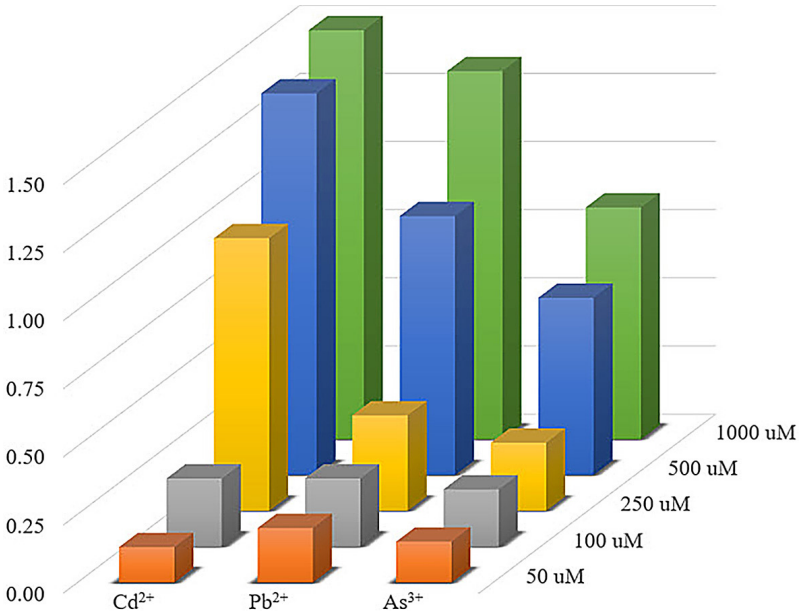

Figure 14. Result of the detection of divalent metal ions and non-trivalent metal ions in water

Cd^{2+} turns slightly bluish, while for Pb^{2+} and As^{3+} it maintains its characteristic color. For more than 500 µM of Cd^{2+}, Pb^{2+} and As^{3+}; the color of the functionalized nanoparticles becomes more clearly bluish after 60 min of the addition of the ions; and when analyzed by UV-Vis spectroscopy, the absorbance peaks range from 518 nm to 700 nm. These results are presented in Figure 14.

The negative potential generated by the analytes in the nanoparticles is due to the cationic nature of the analytes and that L-Cysteine, as a ligand tends to be absorbed with metal ions in times greater than 60 min [Han et al., 2016].

CONCLUSIONS

The production of non-functionalized or reference AuNPs by laser ablation in liquid medium, characterized by UV-Visible spectroscopy, allowed obtaining AuNPs with optical resonance at an average wavelength of 522.84 nm and a diameter of 23.37 nm; presenting a single absorbance maximum peak; therefore, they are spherical nanoparticles [Shafiqa et al., 2018]. From the TEM characterization, it was determined that the nanoparticles have rough surfaces, which makes them suitable for functionalizing with amino acids.

When functionalizing the AuNPs with the linking amino acid L-Cysteine ≥ 97%, there was a resonance displacement of the maximum peak of the wavelength of the spectrum of the functionalized nanoparticles at approximately 22.51 nm; consequently, the increase in diameter at 52.10 nm was produced by the adhesion of the ligand on the metallic surface of the nanoparticles, dispersed by a sonication source at a frequency of 40 KHz for one hour.

The sensitivity of the functionalized nanoparticles was tested for different concentrations of analytes in water; made up of divalent heavy metal ions Cd^{2+}, Pb^{2+}, and trivalent nonmetal As^{3+}. At a concentration greater than 500 uM, the color of the functionalized nanoparticles turned bluish, due to the presence of positive ions; therefore, it was stated that the functionalized nanoparticles detect heavy metals in water.

Acknowledgements

This study was subsidized by the Fondo de Desarrollo Socioeconómico de Camisea (FOCAM) of the Universidad Nacional de Huancavelica. Thanks to the Vice President for Research-UNH and the Faculty of Engineering Electronic-Systems; for the facilities provided, and the support with the necessary infrastructure and equipment.

REFERENCES

1. Arathi, A., Joseph, X., Akhil, V., Mohanan, P.V. 2022. L-Cysteine capped zinc oxide nanoparticles induced cellular response on adenocarcinomic human alveolar basal epithelial cells using a conventional and

organ-on-a-chip approach. Colloids and Surfaces B: Biointerfaces, 211, 112300.

2. Avantes. 2018. Spectrometer UV-Vis-NIR - AvaSpec-ULS2048x64-EVO. https://www.medicalexpo.com/prod/avantes/product-104219-950813.html
3. Awual, M.R., Yaita, T., Suzuki, S., Shiwaku, H. 2015. Ultimate selenium (IV) monitoring and removal from water using a new class of organic ligand based composite adsorbent. Journal of Hazardous Materials, 291, 111–119. https://doi.org/https://doi.org/10.1016/j.jhazmat.2015.02.066
4. Briffa, J., Sinagra, E., Blundell, R. 2020. Heavy metal pollution in the environment and their toxicological effects on humans. Heliyon, 6(9), e04691.
5. Carbajal-Morán, H., Márquez-Camarena, J.F., Galván-Maldonado, C.A. 2022. Influence of Gold Nanoparticles on the Photocatalytic Action of Titanium Dioxide in Physical-Chemical Parameters of Greywater. Journal of Ecological Engineering, 23(1), 182–192. https://doi.org/10.12911/22998993/143942
6. Darbha, G.K., Singh, A.K., Rai, U.S., Yu, E., Yu, H., Chandra Ray, P. 2008. Selective Detection of Mercury (II) Ion Using Nonlinear Optical Properties of Gold Nanoparticles. Journal of the American Chemical Society, 130(25), 8038–8043. https://doi.org/10.1021/ja801412b
7. Demirak, A., Yilmaz, F., Tuna, A.L., Ozdemir, N. 2006. Heavy metals in water, sediment and tissues of Leuciscus cephalus from a stream in southwestern Turkey. Chemosphere, 63(9), 1451–1458.
8. Haiss, W., Thanh, N.T.K., Aveyard, J., Fernig, D.G. 2007. Determination of size and concentration of gold nanoparticles from UV− Vis spectra. Analytical Chemistry, 79(11), 4215–4221.
9. Halkare, P., Punjabi, N., Wangchuk, J., Nair, A., Kondabagil, K., Mukherji, S. 2019. Bacteria functionalized gold nanoparticle matrix based fiber-optic sensor for monitoring heavy metal pollution in water. Sensors and Actuators B: Chemical, 281, 643–651. https://doi.org/https://doi.org/10.1016/j.snb.2018.10.119
10. Han, G., Wang, X., Hamel, J., Zhu, H., Sun, R. 2016. Lignin-AuNPs liquid marble for remotely-controllable detection of Pb 2+. Scientific Reports, 6(1), 1–8.
11. Kateshiya, M.R., George, G., Rohit, J.V, Malek, N.I., Kumar Kailasa, S. 2020. Ractopamine as a novel reagent for the fabrication of gold nanoparticles: Colorimetric sensing of cysteine and Hg2+ ion with different spectral characteristics. Microchemical Journal, 158, 105212. https://doi.org/https://doi.org/10.1016/j.microc.2020.105212
12. Kumari, P., Meena, A. 2020. Green synthesis of gold nanoparticles from Lawsoniainermis and its catalytic activities following the Langmuir-Hinshelwood mechanism. Colloids and Surfaces A: Physicochemical and Engineering Aspects, 606, 125447.
13. Naharuddin, N.Z.A., Abu Bakar, M.H., Sadrolhosseini, A.R., Tamchek, N., Alresheedi, M.T., Abas, A.F., Mahdi, M.A. 2022. Pulsed-laser-ablated gold-nanoparticles saturable absorber for mode-locked erbium-doped fiber lasers. Optics & Laser Technology, 150, 107875. https://doi.org/https://doi.org/10.1016/j.optlastec.2022.107875
14. Quantel. 2019. Q-smart 450 Pulsed Nd:YAG Laser, 213 to 1064nm, 8 to 450mJ, Product - Photonic Solutions, UK. https://www.photonicsolutions.co.uk/product-detail.php?prod=6345
15. Rahman, Z., Singh, V.P. 2019. The relative impact of toxic heavy metals (THMs)(arsenic (As), cadmium (Cd), chromium (Cr)(VI), mercury (Hg), and lead (Pb)) on the total environment: an overview. Environmental Monitoring and Assessment, 191(7), 1–21.
16. Salam, J.A., Vinod, M., Gopchandran, K.G. 2022. Studies on plasmon coupling between pure colloidal gold nanoparticles prepared by laser ablation in water. Materials Today: Proceedings, 54, 882–889. https://doi.org/https://doi.org/10.1016/j.matpr.2021.11.205
17. Seth, R. 2020. L-cysteine functionalized gold nanoparticles as a colorimetric sensor for ultrasensitive detection of toxic metal ion cadmium. Materials Today: Proceedings, 24, 2375–2382.
18. Shafiqa, A.R., Aziz, A.A., Mehrdel, B. 2018. Nanoparticle optical properties: size dependence of a single gold spherical nanoparticle. Journal of Physics: Conference Series, 1083(1), 12040.
19. Shin, M., Yang, S., Kwak, H.W., Lee, K.H. 2022. Synthesis of gold nanoparticles using silk sericin as a green reducing and capping agent. European Polymer Journal, 164, 110960. https://doi.org/https://doi.org/10.1016/j.eurpolymj.2021.110960
20. Sigma-Aldrich. 2019. 1327-53-3. https://www.sigmaaldrich.com/PE/es/search/1327-53-3?focus=products&page=1&perPage=30&sort=relevance&term=1327-53-3&type=product
21. Slocik, J.M., Zabinski Jr, J.S., Phillips, D.M., Naik, R.R. 2008. Colorimetric response of peptide-functionalized gold nanoparticles to metal ions. Small, 4(5), 548–551.
22. Titus, D., Samuel, E.J.J., Roopan, S.M. 2019. Nanoparticle characterization techniques. In Green synthesis, characterization and applications of nanoparticles. Elsevier, 303–319.
23. Tripathi, R.M., Park, S.H., Kim, G., Kim, D.-H., Ahn, D., Kim, Y.M., Kwon, S.J., Yoon, S.-Y., Kang, H.J., & Chung, S.J. 2019. Metal-induced redshift of optical spectra of gold nanoparticles: An instant, sensitive, and selective visual detection of lead ions. International Biodeterioration & Biodegradation, 144,

104740. https://doi.org/https://doi.org/10.1016/j.ibiod.2019.104740

24. Ullah, N., Mansha, M., Khan, I., Qurashi, A. 2018. Nanomaterial-based optical chemical sensors for the detection of heavy metals in water: Recent advances and challenges. TrAC Trends in Analytical Chemistry, 100, 155–166. https://doi.org/https://doi.org/10.1016/j.trac.2018.01.002
25. Waheed, A., Mansha, M., Ullah, N. 2018. Nanomaterials-based electrochemical detection of heavy metals in water: Current status, challenges and future direction. TrAC Trends in Analytical Chemistry, 105, 37–51. https://doi.org/https://doi.org/10.1016/j.trac.2018.04.012
26. Zhang, S., Zhou, H., Kong, N., Wang, Z., Fu, H., Zhang, Y., Xiao, Y., Yang, W., Yan, F. 2021. l-cysteine-modified chiral gold nanoparticles promote periodontal tissue regeneration. Bioactive Materials, 6(10), 3288–3299. https://doi.org/https://doi.org/10.1016/j.bioactmat.2021.02.035